



HAL
open science

Thiabendazole/bentonites hybrids as controlled release systems

Graycyelle R.S. Cavalcanti, Maria G. Fonseca, Edson da Silva Filho, Maguy Jaber

► **To cite this version:**

Graycyelle R.S. Cavalcanti, Maria G. Fonseca, Edson da Silva Filho, Maguy Jaber. Thiabendazole/bentonites hybrids as controlled release systems. *Colloids and Surfaces B: Biointerfaces*, 2019, 176, pp.249-255. 10.1016/j.colsurfb.2018.12.030 . hal-02169301

HAL Id: hal-02169301

<https://hal.sorbonne-universite.fr/hal-02169301v1>

Submitted on 1 Jul 2019

HAL is a multi-disciplinary open access archive for the deposit and dissemination of scientific research documents, whether they are published or not. The documents may come from teaching and research institutions in France or abroad, or from public or private research centers.

L'archive ouverte pluridisciplinaire **HAL**, est destinée au dépôt et à la diffusion de documents scientifiques de niveau recherche, publiés ou non, émanant des établissements d'enseignement et de recherche français ou étrangers, des laboratoires publics ou privés.

1 **Thiabendazole/bentonites hybrids as controlled release**
2 **systems**

3
4 Graycyelle R. S. Cavalcanti^{1,3}, Maria G. Fonseca^{1*}, Edson C. da Silva Filho² and Maguy
5 Jaber^{*3}

6
7 ¹*Núcleo de Pesquisa e Extensão - Laboratório de Combustíveis e Materiais (NPE -*
8 *LACOM). Universidade Federal da Paraíba, Cidade Universitária, s/n - Castelo*
9 *Branco III, 58051-085, João Pessoa - PB, Brazil.*

10 ²*Interdisciplinary Laboratory of Advanced Materials, CCN, UFPI, 64049-550,*
11 *Teresina, Piauí, Brazil,*

12 ³*Sorbonne Université, Laboratoire d'Archéologie Moléculaire et Structurale, CNRS*
13 *UMR 8220, Tour 23, 3ème étage, couloir 23-33, BP 225, 4 place Jussieu, 75005 Paris,*
14 *France.*

15
16
17
18
19
20
21
22
23
24
25
26
27
28 The manuscript includes 4432 words, 6 figures and 2 tables

29 **Highlights**

- 30 • Thiabendazole intercalates in the interlamellar space of bentonite.
31 • The nature of the interlamellar cation influenced the adsorption capacity of
32 bentonite.
33 • Release tests showed that part of the drugs are still adsorbed on the bentonites.
34 • The solids have shown to be promising for pharmaceutical applications.

35

36 **Abstract**

37 Clay minerals are commonly used in pharmaceutical products as excipients and active
38 agents. New drug vehicles based on clay minerals have been developed. In this work,
39 sodium (BentNa), calcium (BentCa) and magnesium (BentMg) exchanged bentonites
40 were used for the sorption of thiabendazole (TBZ), and their potential use as controlled
41 release systems was evaluated. Pristine bentonite and exchanged bentonites were
42 characterized by X-ray diffraction, infrared spectroscopy, thermogravimetry and
43 transmission electron microscopy (TEM), and the influence of the different parameters
44 such as pH, contact time and initial concentration of the drug was investigated. The
45 maximum adsorption reached after 45 min period with 2000 mg L⁻¹ of thiabendazole to
46 BentNa and after 105 min with 1300 mg L⁻¹ to BentCa and BentMg, respectively. The
47 maximum adsorbed quantities of thiabendazole were 164.4; 152.3 and 133.3 mg g⁻¹ for
48 BentNa, BentCa and BentMg, respectively. The emission profiles obtained for the
49 bentonite/drug hybrids were similar when simulated body fluids were used and these
50 emission profiles were fitted according to the Korsmeyer-Peppas kinetic model.

51

52 **Keywords:** *Clay minerals, Drug delivery system, thiabendazole, clay/drugs hybrids*

53

54

55

56

57 The manuscript includes 4432 words, 6 figures and 2 tables

58

59 **1. Introduction**

60 Clay minerals are an important class of natural materials which are used in
61 traditional medicine [1], their biological uses having been reported since antiquity. The
62 medicinal properties of clay minerals have long been recognized in indigenous cultures,
63 and their use in traditional medicine confined mainly to external applications for the
64 treatment of skin problems and gastrointestinal diseases [2].

65 The specific physical and chemical properties of clay minerals such as
66 adsorption, cation exchange capacity, swelling capacity, ability to form colloidal
67 solutions, optimum rheological behavior and dispersibility in water [3-6] as also their
68 low cost, abundance, biocompatibility versatility and effectiveness, have resulted, in
69 recent decades, in the introduction of these minerals, into various technological
70 processes [7-16] Clay minerals have therefore now been introduced as components in
71 various pharmacological formulations, in which they are used as excipients. In addition
72 to classic pharmaceutical uses, they can also be employed in the development of new
73 drug delivery systems (DDS) [17-19]

74 Although all pharmaceutical dosage forms can be considered to DDS (since
75 they use the administration of drugs intended to reach a site of action and maintain a
76 certain concentration over the entire period of treatment), the final therapeutic effect of
77 a pharmaceutical treatment will depend on several factors, which will involve the nature
78 of the drug as well as the form taken for its administration and dosage [2,18]. Thus, the
79 development of new technologies which aim to reduce the quantity of the administered
80 dose and decrease the levels of drug toxicity, has led to new controlled release systems
81 [20].

82 The formation of drug/clay mineral hybrids can influence the bioavailability of
83 the drug, the release rate, and the chemical stability of the systems [17]. For example,
84 stronger drug/bentonite interactions resulted in slower release and lower rates of drug
85 absorption and, in consequence, the reduction of the plasma concentration of the drug
86 [2,21]. These properties are not desirable for drugs such as antihistamines, which
87 require an immediate therapeutic concentration in the blood. Clay minerals are however
88 highly recommended as carriers for drugs that require slow and prolonged release, such
89 as antibiotics (amoxicillin, tetracycline, cephadrine, metronidazole and gentamicin),
90 antihypertensive drugs (propranolol, nifedipine, amlodipine, etc.) and antipsychotics
91 (aripiprazole, buspirone) [22]. Thiabendazole (TBZ) is an anthelmintic and antifungal
92 drug used in the treatment of fungal and worm infections in animals and humans [23].

93 Four different TBZ species can be generated by protonation–deprotonation reactions
94 depending on the pH of the solution [24].

95 Previous studies have studied the adsorption of TBZ on Argentine clay,
96 [25,26]. It was observed that there was a drastic reduction in TBZ adsorption when the
97 pH was changed from 5 to 7, as a result of the presence of uncharged thiabendazole
98 species. Moreover, at a pH lower than 2, the ion exchange is the main mechanism of
99 adsorption. Aluminum pillared montmorillonite was also used as a TBZ adsorbent in an
100 aqueous medium [23,24].

101 The use of bentonite and thiabendazole for the development of controlled
102 release systems has also been reported; Yasser (2014) used Ca-Bentonite in controlled
103 release formulation of TBZ for reduced contaminations to soil water. Results showed
104 that TBZ was better adsorbed in clay at the value pH 3 and the release experiments
105 showed that liberation the TBZ that slower at pH 3 than at pH 5.5 or pH 9.

106 This present work focused on the study of the thiabendazole/bentonites system
107 for drug delivery, the aim being the investigation of the influence of the interlayer
108 cations of bentonite on the interaction with thiabendazole. The kinetics of *in vitro*
109 release of thiabendazole from hybrids in simulated gastric (SGF), body (SBF) and
110 intestinal (SIF) fluids were also determined.

111

112 **2. Experimental**

113 *2.1 Material and chemicals*

114 The bentonite sample was donated by the Bentonisa do Nordeste SA in Brazil
115 (Boa Vista, PB).. The sample presented a cationic exchange capacity (CEC) of 88 cmol
116 (+) Kg⁻¹ and the following chemical composition - SiO₂ (52.98%), Al₂O₃ (18.35 %),
117 Fe₂O₃ (3.96%), MgO (2.47%), Na₂O (2.56%), K₂O (0.22%), with a loss ignition of
118 18.59%.

119 Thiabendazole (2-(thiazol-4-yl) benzimidazole, M = 201.3 gmol⁻¹, pKa 2.5,
120 4.7 and 12.0), was acquired from Sigma-Aldrich, (99% analytical grade). Thiabendazole
121 is partially soluble in water (28 mg L⁻¹) and soluble in acid solutions at low
122 concentrations; [23, 25, 26], a solution of the drug was therefore prepared with 3000 mg
123 L⁻¹ drug solution in 0.01 mol L⁻¹ HCl. All the samples prepared were dried at 343 K for
124 48 h and then conducted for characterization.

125 *2.2 Ion exchange*

126 Raw bentonite (Bent) was purified to remove quartz by the centrifugation
127 decantation method. The sample was suspended in 1.0 mol L⁻¹ NaCl, CaCl₂·2H₂O or
128 MgCl₂·6H₂O solutions, and was maintained under orbital agitation at 300 K. The same
129 procedure was repeated twice to guarantee the process of ion exchange [3]. The
130 exchange samples were named BentNa, BentCa and BentMg.

131 *2.3 Sorption of thiabendazole*

132 We first monitored the influence of pH on the drug-bentonites interaction.
133 Samples of 200 mg of each exchange solid was suspended in 50.0 mL of 500 mg L⁻¹
134 drug solution, and the pH was adjusted to 1.4, 2.3 and 3.8, the values of which were
135 determined based on the pKa of thiabendazole. The suspension was stirred for a period
136 of 24 h. The final solids were centrifuged, and the thiabendazole in equilibrium solution
137 was quantified by UV-Vis molecular spectrometry in an UV-Vis spectrofotometer
138 Shimadzu model 2550, at 298 nm in the concentration range of 2 – 8 mg L⁻¹.

139 The sorbed drug on solid (q_e) was calculated by equation (1).

140

141
$$q_e = \frac{(C_0 - C_e)V}{m} \quad (1)$$

142 Where C_0 and C_e are the drug concentration (mg L⁻¹) in solution before and after
143 sorption respectively, V (L) is the volume of the drug solution, and m (g) is the mass of
144 the bentonite.

145 To investigate the influence of time on adsorption, the same procedure was used,
146 and the time was varied between 0 and 120 min in the same conditions.

147 The effect of the initial concentration of the drug was monitored by using
148 thiabendazole at 30 and 3000 mg L⁻¹, which reacted with bentonites at optimum
149 conditions for both pH and time.

150 *2.4. Synthesis of bentonite/drug hybrids*

151 The synthesis of the hybrids was carried out basing oneself on the previous
152 conditions of pH, time and drug concentration, as determined in the adsorption tests.
153 Therefore, a 1.0 g sample of each bentonite category was suspended in 250 mL of 2000
154 mg L⁻¹ drug solution, and then reacted for a period of 45 min in the case of the sodium

155 bentonite, and for the calcium and magnesium samples, 1.0 g of each solid was reacted
156 with the 1300 mgL⁻¹ drug solution for 105 min. The systems were maintained under
157 orbital agitation at 300 K. Finally, the drug concentration was determined as described
158 above.

159

160 2.5. Release test

161 For the release test, simulated gastric (SGF, HCl aqueous solution, pH 1.2), body
162 (SBF, pH 7.4) and intestinal (SIF, phosphate buffer solution, pH 7.4) fluids were
163 prepared. The SBF was prepared by dissolving the following chemical reagents in 1.0 L
164 distilled water: NaCl (7.996 g), NaHCO₃ (0.350 g), KCl (0.224 g), K₂HPO₄·3H₂O
165 (0.228 g), MgCl₂·6H₂O (0.305 g), CaCl₂ (0.278 g), Na₂SO₄ (0.071 g), NH₂C(CH₂OH)₃
166 (6.057 g) [27].

167 The release test followed standard procedure where 0.1 g of each solid
168 BentNaTBZ, BentCaTBZ and BentMgTBZ was suspended as a disk in 400 cm³ of each
169 fluid. The system was maintained at 335 K for 72 h, and at each time interval, aliquots of
170 5.0 mL of the solution were removed, and the same volume of drug solution then added
171 to the suspension [28].

172 The drug concentration was quantified as described above. The cumulative
173 drug concentration was calculated (C_c) as determined in Equation (2), where C_f (mg L⁻¹)
174 is the final drug concentration in solution, V_f and V_a (L) are the volumes of fluid and
175 aliquota, respectively.

$$176 \quad C_c = C_f + \frac{(V_a * C_f)}{V_f} \quad (2)$$

177

178 3. Results and discussion

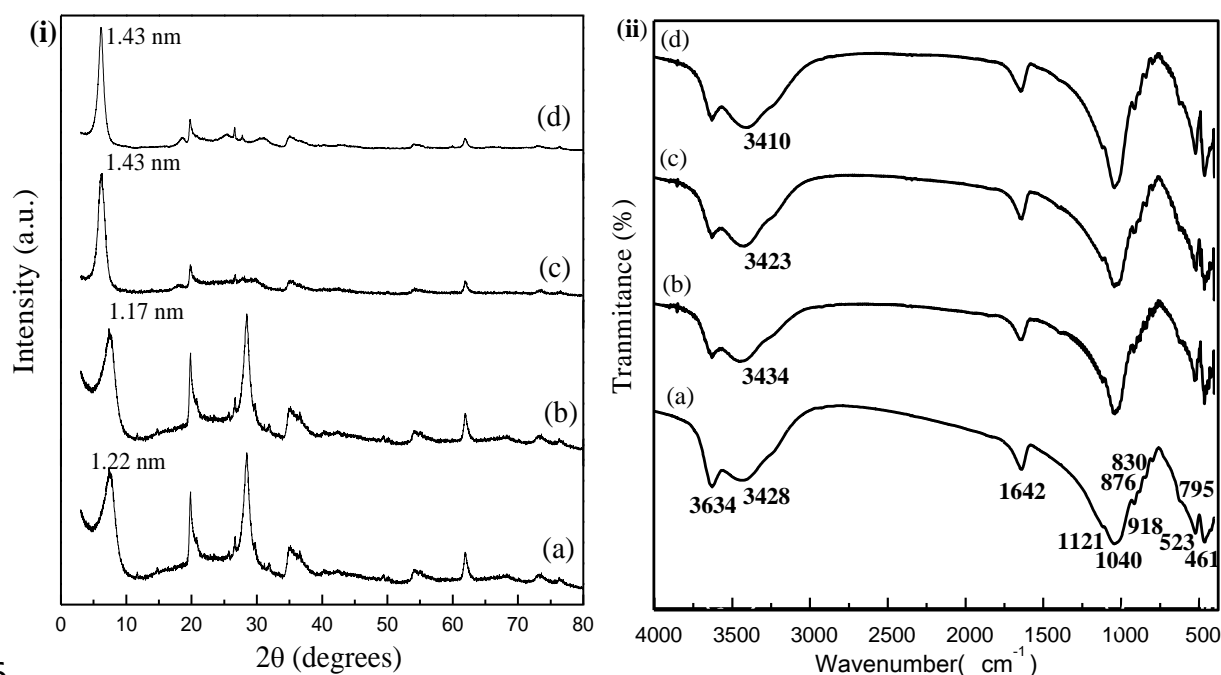
179 3.1 Characterization of exchanged bentonites

180 For raw bentonite, the XRD patterns of the samples (SM1) exhibited the
181 principal montmorillonite reflection at 2θ 7.24° ($d_{001} = 1.22$ nm) [30]. Other reflections
182 were observed at 2θ 19.8°; 28.5°; 34.9° and 61.8° and were indexed to montmorillonite
183 phase in agreement with ICDD file 00-060-0318. The additional peaks at 2θ 11.7° and

184 26.5° were associated to muscovite and quartz phases, respectively. After removal of
185 the quartz, the XRD patterns maintained the reflections of montmorillonite, and the
186 quartz peaks were not observed.

187 After ion exchange, the samples displayed reflections at 7.55°, 6.19° and 6.17°
188 associated to the (001) plan with basal spacings of 1.17, 1.43 and 1.43 nm for BentNa,
189 BentMg and BentCa respectively. These values are in agreement with those observed
190 for natural sodium [30], calcium [31] and magnesium montmorillonites [32]. In the Bent
191 and BentNa samples, an additional peak at 28.4° is attributed to the presence of residual
192 NaCl in according ICDD file 01-083-1728. The higher values of the basal spacings were
193 those obtained for samples with higher hydration cation volume, 156.7 and 176.9 cm³
194 mol⁻¹ for Ca²⁺ and Mg²⁺, and 109.0 cm³ mol⁻¹ for Na⁺.

195 FTIR spectra (Figure 1ii) for all samples displayed bands at 3634 cm⁻¹, assigned
196 to structural OH stretching (M-OH, M = Al³⁺, Mg²⁺, Fe³⁺), and at 3400 cm⁻¹ resulting
197 from OH stretching of interlayer water and silanol (Si-OH); the OH stretching of water,
198 however, showed a small variation which can be related to the interlayer cation. The
199 band associated to the bending of water was observed at 1642 cm⁻¹ [33, 34]. Other bands
200 were detected at 1121 and 1040 cm⁻¹ and assigned to Si-O asymmetric and symmetric
201 stretchings, respectively. Si-O-Al and Si-O-Si bending vibrations, were detected at 523
202 and 461 cm⁻¹ respectively. Isomorphic substitution of Al³⁺ for Mg²⁺ and Fe²⁺ in the
203 octahedral sheet provokes changes in the OH deformation bands at 918 cm⁻¹ (Al-Al-
204 OH), 876 cm⁻¹ (Al-Fe-OH) and 830 cm⁻¹ (Al-Mg-OH), and these were dependent on the
205 nature of the cation present [35,36].



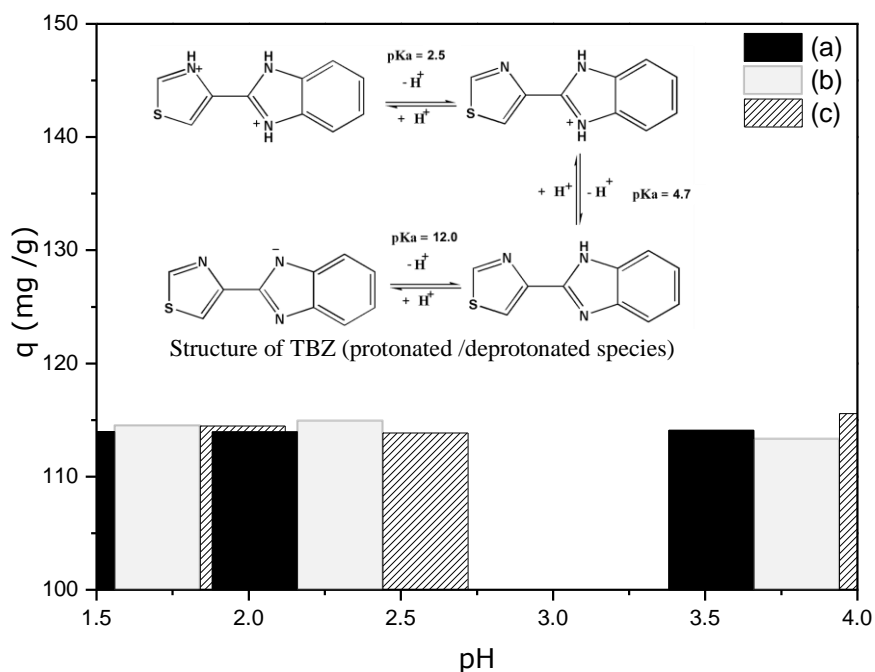
206

207 Figure 1 i) XRD patterns and ii) FTIR spectra for (a) Bent, (b) BentNa, (c) BentCa and
 208 (d) BentMg.

209 In the DTG curves for BentNa, BentCa and BentMg (Figure SM2), two mass
 210 losses were observed: at 298-660 K and at 660-1200 K for BentNa.. The first is related
 211 to the loss of physically adsorbed water and interlayer water, and the second is the result
 212 of the dehydroxilation and loss of the coordination water. In the instance of the
 213 magnesium and calcium bentonites, three mass losses were observed, at 298-573,573-
 214 754 K and 754-1200 K for BentCa, and at 298-483 K, 483-748 K and 748-1200 K for
 215 BentMg. As above, the first loss is related to the loss of adsorbed and interlayer waters,
 216 and the second and third ones can be assigned to the dehydroxilation and loss of
 217 coordination water, respectively. [30,37]

218 3.2 Sorption of thiabendazole

219 The effect of pH on thiabendazole sorption onto BentNa, BentCa and BentMg
 220 (Figure 2), showed a maximum sorption of 114 mg g⁻¹ for all pH values. Therefore, the
 221 value of 1.4 was used in all experiments. The thiabendazole molecules are present at 92
 222 % for TBZ⁺⁺ species (pKa = 2.5) and 99.9 % for TBZ⁺ (pKa = 4.7). The sorption of
 223 thiabendazole is usually pH-dependent [26]. For protonated TBZ (TBZ⁺), the sorption
 224 onto bentonite occurred by ion exchange between the inorganic cation in the interlayer
 225 space and the organic one, TBZ⁺ [38].

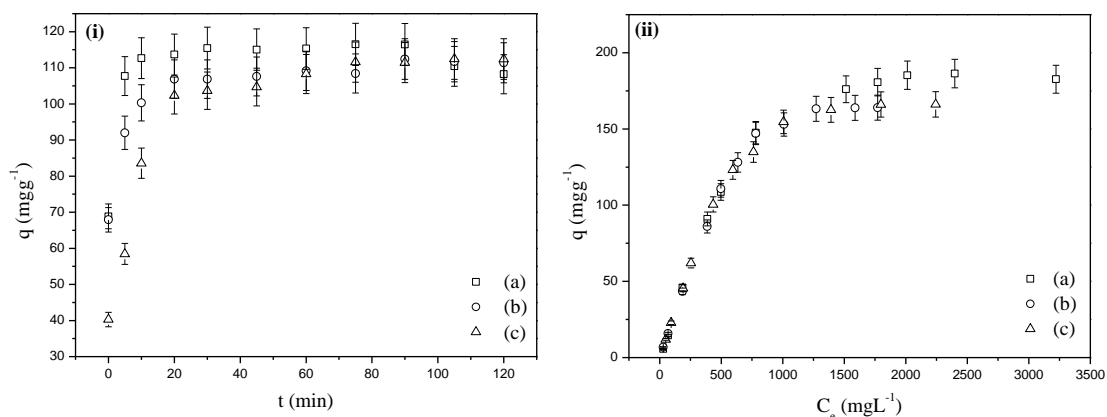


226

227 Figure 2. The effect of pH on thiabendazole adsorption onto (a) BentNa, (b) BentCa and
 228 (c) BentMg at 300 K. Inserted figure is that of the TBZ structure.

229 The influence of contact-time on sorption of thiabendazole onto bentonites
 230 (Figure 3i), displayed equilibrium at 30, 90 and 75 min where the maximum sorption
 231 capacities were 115.5; 111.5 and 111.6 mg g⁻¹ for BentNa, BentCa and BentMg
 232 respectively. The data were fitted to second order kinetics (Figure SM3 and Table 1).

233 The equilibrium isotherms (Figure 3ii) show that the maximum adsorbed
 234 quantities are observed at a 2000 mg L⁻¹ for Na-Bent with 185 mg g⁻¹ of Thiabendazole,
 235 while for CaBent and Mg-Bent 163 mg g⁻¹ were adsorbed from a starting concentration
 236 of 1300 mg L⁻¹. The experimental data were better fitting to the Langmuir than the
 237 Freundlich model (Figures SM4.1 and SM4.2), and the resulting parameters are
 238 presented in Table 1.



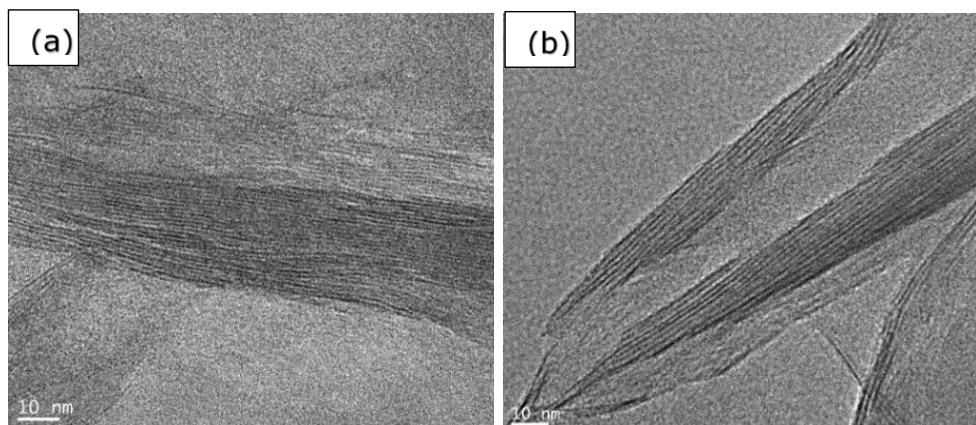
239

240 Figure 3. i) Effect of time and ii) initial drug concentration on thiabendazole adsorption
 241 on (a) BentNa (b) BentCa and (c) BentMg at 300 K and pH 1.4.

242 3.3 Characterization of thiabendazole/bentonite hybrids

243 CHN elemental analysis gave the following results: 164.4; 152.3 and 133.3 mg
 244 g^{-1} of the drug on BentNaTBZ, BentCaTBZ and BentMgTBZ, respectively. XRD
 245 patterns (Figure SM5) showed basal spacings altered from 1.17 nm to 1.42 nm in
 246 BentNaTBZ, 1.52 nm to 1.41 nm in BentCaTBZ, and 1.43 nm to 1.39 nm in
 247 BentMgTBZ. In other words, while for the sodium sample the basal spacing had a
 248 higher value, the values decreased for the other two samples, suggesting some loss of
 249 water in the intercalation of the organic molecule.

250 TEM micrographs (Figure 4, Figure SM6) suggested the typical layered
 251 arrangement of pristine bentonites with interlayer spacings of 1.15-1.23 nm for BentNa;
 252 1.44-1.56 nm for BentCa and 1.41-1.49 for BentMg. The solids saturated with the drug
 253 presented a similar morphology [31,39] and the interplanar spacings were 1.31-1.47 nm
 254 for BentNaTBZ, BentCaTBZ and BentMgTBZ, this data in agreement with the XRD
 255 patterns (Figure 4).



256

257 Figure 4. TEM micrographs of (a) BentNa and (b) BentNaTBZ

258 Taking into consideration the size of thiabendazole (1.15 nm x 0.72 nm x 0.34
259 nm) [25], the thickness of the montmorillonite (1.35 nm) [30] the XRD patterns and
260 TEM images, the interaction of thiabendazole and bentonite can be seen to be in
261 preponderance through an ion exchange mechanism, involving also the intercalation of
262 the protonated drug in the inter-layer spacing of montmorillonite [26,27].

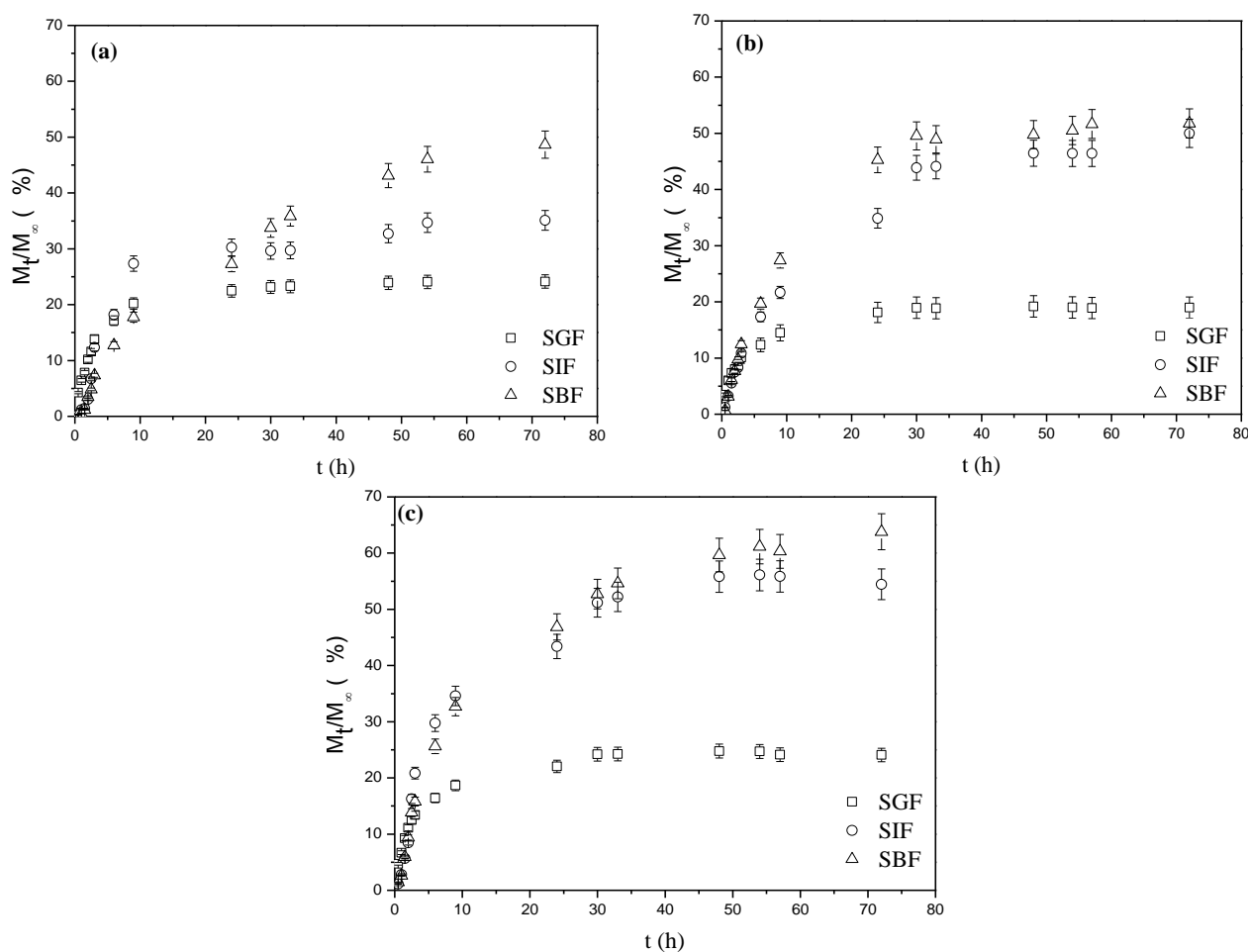
263 The FTIR spectra of the hybrids presents typical bands of the free drug (Figure
264 SM7). However, the bands assigned to C-N and N-H have shifted from 1306 to 1313
265 cm^{-1} possibly as a result of the protonation of the nitrogen of the benzimidazole group,
266 and from 1574 to 1603 cm^{-1} , suggesting the presence of the TBZ^+ and TBZ^{++} forms on
267 the bentonite [27, 40].

268 UV-VIS spectra for the exchanged samples BentNa, BentCa and BentMg
269 (Figura SM8) displayed a broadadsorption at 250-300 nm, assigned to O→Si and
270 O→Al charge transfer bands [41]. After drug loading, a band centred at 298 nm was
271 detected and this was the same as that observed for the free drug, which is associated to
272 the $n\text{-}\pi$ and $\pi\text{-}\pi^*$ molecular orbitals of the TBZ.

273 3.4 Release test

274 The release of thiabendazole from hybrids at the solid/liquid interface involved a
275 number of processes which promote the transport of the drug from the solid to the liquid
276 phase. Specifically, for clay minerals, diffusion is relevant and includes drug desorption
277 from the external surface, and the loss of the intercalated molecules from the interlayer
278 region [18].

279 The release curves for thiabendazole from the three samples over a period of 72
 280 h in the simulated fluids (Figure 5), indicate a similar behavior with a release of 20, 27
 281 and 17 % in the first 9 h for BentNaTBZ; 14, 21 and 27 % for BentCaTBZ and 18, 34
 282 and 32 % for BentMgTBZ SGF, SIF and SBF fluids, respectively. The slow and
 283 controlled release is associated to cationic exchange between the intercalated charged
 284 drug and the alkaline cations from the simulated fluids [42]



285
 286 Figure 5. Cumulative release profiles of (a) BentNaTBZ, (b) BentCaTBZ and (c)
 287 BentMgTBZ

288

289 The quantity of released TBZ species was 100% lower, probably as a result of an
 290 equilibrium process in the ion exchange which is a complete reaction [42]. Furthermore,
 291 electrostatic interaction between the cations and the anionic charge of the
 292 montmorillonite results in incomplete release [43].

293 The release data were adjusted to Korsmeyer-Peppas model (Equation 3),

294
$$\frac{M_t}{M_\infty} = kt^n \quad (3)$$

295 Where M_t/M_∞ is the fractional release of the drug at time t , and k and n kinetic
296 constants. The n value is used to characterize the principal mechanism of drug release;
297 where release is Fickian diffusion when $n \leq 0.45$, if $0.45 \leq n \leq 0.89$, it indicates
298 anomalous (non-Fickian) transport, if $n = 0.89$ the release follows case II and $n > 0.89$
299 super case II transport [44]

300 The obtained kinetic parameters (Figure SM9) for the system under investigation
301 are presented in Table 2.

302 The values of R^2 indicate a good adjustment of the data for BentMgTBZ and
303 BentCaTBZ in the three simulated fluids. The n values were in the range of $0.45 < n <$
304 0.89 for the release in SGF in all systems, indicating that diffusion and erosion were the
305 main mechanisms at play in the kinetic process of release. It is important to note that
306 this model was proposed for polymers, and therefore the erosion cannot be considered
307 reasonable for a clay mineral matrix [46]

308 For the TBZ release SIF and SBF, the values of n were 0.89 suggesting that the
309 kinetics of the reaction are based on a super case II transport mechanism, where the
310 diffusion rate of the solvent is higher than the relaxation rate, and the drug release
311 mechanism occurs as a result of swelling and stresses [47].

312 The XRD patterns of the solids after the release test (Figure SM10) showed that
313 the basal spacings were lower than the initial values observed for the loaded samples: ie.
314 1.42 nm for Bent Na, 1.41 nm for BentCa, and 1.39 nm for BentMg, suggesting the
315 presence of the unreleased drug in the final solids.

316

317 **4. Conclusion**

318 Thiabendazole was loaded onto three exchanged bentonites at different
319 conditions of equilibrium for 45 min and at an initial drug concentration of 2000 mgL^{-1}
320 for BentNa, and for 105 min at an initial drug concentration of 1300 mgL^{-1} for BentCa
321 and BentMg.

322 The loaded solids behaved as good drug *in vitro* release systems in simulated
323 fluids, with SBF having the highest release of the three samples. The BentMgTBZ

324 system exhibited the highest cumulative release compared with the other samples. The
325 thiabendazole release kinetics of the drug/bentonite hybrids were similar, and adjusted
326 to the Korsmeyer-Peppas model.

327 The different tests demonstrated that the nature of the interlayer cation in
328 bentonite influenced the thiabendazole loading and release quantities, and that it is a key
329 parameter that should be considered in the application of bentonites as vehicles for
330 drugs.

331 **Acknowledgments**

332 CNPq is acknowledged for research fellowships to M.G. Fonseca and E.C. Silva
333 Filho. G.R.S. Cavalcanti thanks to CAPES for providing research fellowship.
334 CAPES/COFECUB (835/2015) for financial support.

335 **References**

- 336
337 1. Abrahams P. W. Involuntary Soil ingestion and geophagia: a source and sink of
338 mineral nutrients and potentially harmful elements to consumers of earth
339 materials. *Applied Geochemistry*, 2012, 27,954–968.
- 340 2. Ghadiri. M., Chrzanowski. W., Rohanizadeh. R. Biomedical applications of
341 cationic clay minerals. *Royal Society of Chemistry*, 2015, 5, 37, 29467–29481.
- 342 3. Bergaya. F. Lagaly. G. General Introduction: Clays. *Clay Minerals and Clay*
343 *Science*. In: Bergaya. F. Theng. B. K. G. Lagaly. G. Eds., *Handbook of Clay*
344 *Science*. Elsevier. Amsterdam. *Developments in clay science*, 2013, 5,1-19.
- 345 4. Brigatti. M. F., Galán. E., Theng. B. K. G. Structure and mineralogy of clay
346 minerals. In: Bergaya. F. Theng. B. K. G. Lagaly. G. Eds., *Handbook of clay*
347 *science*. Elsevier. Amsterdam. *Developments in clay science*, 2013, 5,21-81.
- 348 5. Tangaraj, V.et al., Adsorption and phytophysical properties of fluorescent dyes
349 over montmorillonite and saponite modified by surfactant, *Chemosphere*, 2017,
350 184, 1355-1361.

- 351 6. Jaber, M. et al. Selectivities in adsorption and peptidic condensation in the
352 (arginine and glutamic acid)/montmorillonite clay system, *J. The Journal of*
353 *Physical Chemistry C*, 2014, 118 (44), 25447–25455.
- 354 7. He, H. et al. Silylation of clay mineral surfaces. *Applied Clay Science*, 2013, 71,
355 15–20.
- 356 8. Fournier, F. et al. Physico-chemical characterization of lake pigments based on
357 montmorillonite and carminic acid, *Applied Clay Science*, 2016, 130, 12-17.
- 358 9. Gomes, S.S. et al. Silylation of leached-vermiculites following reaction with
359 imidazole and copper sorption behaviour, *Journal of hazardous materials*, 2016,
360 306, 406-418.
- 361 10. Trigueiro, P. et al. Going through wine fining : intimate dialogue between
362 organics and clays, under revision, *Colloids and surfaces b : biointerfaces*, 2018,
363 166, 1 2018, 79-88.
- 364 11. Zhuang, G. et al. Enhancing the rheological properties and thermal stability of
365 oil-based drilling fluids by the synergetic use of organo-montmorillonite and
366 organo-sepiolite, 2018, *Applied Clay Science*, 2018, 161, 505-512.
- 367 12. Guillermin, D. et al. New Pigments Based On Carminic Acid And Smectites, A
368 Molecular Investigation, *Pigments And Dyes*, 2019, 160, 971-982.
- 369 13. Trigueiro, P. et al. Intimate dialogue between anthraquinone dyes and pillared
370 clay minerals, *Pigments and dyes*, 2018, 159, 384-394.
- 371 14. Zhuang, L. et al. Comparative study on the structures and properties of organo-
372 montmorillonite and organo-palygorskite in oil-based drilling fluids, *Journal of*
373 *industrial and chemical engineering*, 2017, 56, 248-257.

- 374 15. Pereira, F. A.R., et al. Green biosorbent based on chitosan-montmorillonite
375 beads for anionic dyes removal, *Journal of Environmental Chemical*
376 *Engineering*, 2017, 4(5), 3309-3318.
- 377 16. El Adraa, K. et al. Montmorillonite-cysteine composites for heavy metal cation
378 complexation: a combined experimental and theoretical study, *Chemical*
379 *Engeneering Journal*, 2017, 314, 406-417.
- 380 17. Rodrigues. L. A. De S. et al. The Systems containing clays and clay minerals
381 from modified drug release: a review. *Colloids and Surfaces B: Biointerfaces*,
382 2013, 103,642–651.
- 383 18. Viseras. C. et al. Current challenges in clay minerals for drug delivery. *Applied*
384 *Clay Science*, 2010, 48,3, 291–295.
- 385 19. Bouaziz, Z. et al. dual role of layered double hydroxide nanocomposites on
386 antibacterial activity and degradation of tetracycline and oxytetracyline,
387 *Chemosphere*, 2018, 2016, 175-183.
- 388 20. Shen. J. et al. Mucoadhesive effect of thiolated peg stearate and its modified nlc
389 for ocular drug delivery. *Journal of Controlled Release*,2010,137,217-223.
- 390 21. Ruiz- Hitzky. E., Aranda. P., Darder. M. Hybrid and biohybrid materials based
391 on layered clays. In: Brunet. E., Colón. J. L., Clearfield A. Eds. *Tailored*
392 *Organic-Inorganic Materials*,Wiley, 2015, 245-297.
- 393 22. Yang. J. H. et al. Drug-Clay nanohybrids as sustained delivery systems. *Applied*
394 *Clay Science*,2016,130, 20-32.
- 395 23. Roca Jalil. M. E. et al. Improvement in the adsorption of thiabendazole by using
396 aluminum pillared clays. *Applied Clay Science*, 2013, 71,55–63.
- 397 24. Roca Jalil, M. E. et al. Effect of the al/clay ratio on the thiabendazol removal by
398 aluminum pillared clays. *Applied Clay Science*,2014, 87, 245–253.

- 399 25. Yasser Z. E-N. Development of controlled release formulations of thiabendazole
400 Journal of Agricultural Chemistry and Environment,2014,3,1-8.
- 401 26. Lombardi. B., Baschini. M., Torres Sánchez. R. M. Optimization of parameters
402 and adsorption mechanism of thiabendazole fungicide by a montmorillonite of
403 north Patagonia. Applied Clay Science, 2003, 24, 1–2, 43–50.
- 404 27. Lombardi. B. M. et al. Interaction of thiabendazole and benzimidazole with
405 montmorillonite. Applied Clay Science,2006, 33, 1, 59–65.
- 406 28. Xu, W. et al. Controllable release of ibuprofen from size-adjustable and surface
407 hydrophobic mesoporous silica spheres. Powder Technology, 2009,191,1–2, 13–
408 20.
- 409 29. Joshi, G. V. et al. Montmorillonite as a drug delivery system: intercalation and
410 in vitro release of timolol maleate. International Journal of Pharmaceutics,374,
411 1–2, 53–57, 2009a.
- 412 30. Lagaly, G., Ogawa, M., Dékány, I. Clay Mineral-Organic. Em: Bergaya, F.,
413 Theng, B. K. G., Lagaly, G., Eds., Handbook of Clay Science. Elsevier,
414 Amsterdam. Developments In: Clay Science, 2013,5, 435-505.
- 415 31. Sun. Z. et al. XRD, TEM and Thermal analysis of Arizona ca-montmorillonites
416 modified with didodecyldimethylammonium bromide. Journal of Colloid and
417 Interface Science, 2013, 408,1,75–81.
- 418 32. Paz, S. P. A., Angélica, R. S., De Freitas Neves, R. Mg-bentonite in the
419 parnaíba paleozoic basin, northern Brazil. Clays and Clay Minerals, 2012,
420 60,3,265–277.
- 421 33. Madejová. J. FTIR Techniques in clay mineral studies. Vibrational
422 Spectroscopy, 2003,31, 1,1–10.

- 423 34. Tyagi. B., Chudasama. C. D., Jasra. R. V. Determination of structural
424 modification in acid activated montmorillonite clay by FT-IR spectroscopy.
425 Spectrochimica Acta - Part A: Molecular and Biomolecular Spectroscopy,2006,
426 64,2,273–278.
- 427 35. Wu, L. M. et al. Fourier Transform Infrared spectroscopy analysis for
428 hydrothermal transformation of microcrystalline cellulose on montmorillonite.
429 Applied Clay Science,2014, 95,74–82.
- 430 36. Petit. S., Madejova J. Fourier Transform Infrared Spectroscopy. In: Bergaya. F.
431 Theng. B. K. G. Lagaly. G. Eds., Handbook of Clay Science. Elsevier.
432 Amsterdam. Developments in Clay Science, 2013, 5,213-231.
- 433 37. Földvári. M. Handbook of The Thermogravimetric system of minerals and its
434 use in geological practice. Central European Geology, 2011,56, 1-179.
- 435 38. Roca Jalil. E. Desarrollo de arcillas pilareadas con al a partir de una bentonita
436 natural de la norpatagonia argentina para la remoción de tiabendazol. Msc.
437 Thesis. Universidad Nacional De San Luis. San Luis. Argentina. 2010.
- 438 39. Park. Y., Ayoko. G. A., Frost. R. L. Characterisation of organoclays and
439 adsorption of p-nitrophenol: environmental application. Journal of Colloid and
440 Interface Science,2011,360, 2,440–456.
- 441 40. Lin-Vien. Daimay. et al. The Handbook of Infrared and Raman characteristic
442 frequencies of organic molecules. Academic Press,1991. San Diego.
- 443
- 444 41. Zaki, M. I. et al. Ceria on silica and alumina catalysts: dispersion and surface
445 acid- base properties as probed by x-ray diffractometry, UV-Vis diffuse
446 reflectance and in situ IRadsorption studies. Colloids and Surfaces A:
447 Physicochemical and Engineering Aspects,1997,127, 1–3, 47–56.

- 448 42. Joshi, G. V. et al. Montmorillonite intercalated with vitamin B1 as drug carrier.
449 Applied Clay Science, 2009b,45, 4,248–253.
- 450 43. Nunes, C.D.et al. Load- Ing and delivery of sertraline using inorganic micro and
451 mesoporous materials. European Journal Pharmaceutics Biopharmaceutics,
452 2007,66,357–365.
- 453 44. Mhlanga, N., Ray, S. S. Kinetic models for the release of the anticancer drug
454 doxorubicin from biodegradable polylactide/metal oxide-based hybrids.
455 International Journal of Biological Macromolecules, 2015,72,1301–1307.
- 456 45. Golubeva, O. Y., Pavlova, S. V., Yakovlev, A. V. Adsorption and in vitro
457 release of vitamin b1 by synthetic nanoclays with montmorillonite structure.
458 Applied Clay Science, 2015,112–113,10–16.
- 459 46. Peppas, N.A., Bures, P., Leobandung, W., Ichikawa, H. Hydrogels in
460 pharmaceutical formulations. European Journal Pharm. Biopharm,200,50, 27–
461 46.
- 462 47. Munday, D.L, Cox, P.J. Compressed xanthan and karaya gum matrices:
463 hydration, erosion and drug release mechanisms. International Journal of
464 Pharmaceutics,2000,2031-2,179-192.
- 465 48. Tümsek. F., Avci. Ö. Investigation of kinetics and isotherm models for the acid
466 orange 95 adsorption from aqueous solution onto natural minerals. Journal of
467 Chemical and Engineering Data,2013,58,3,551–559.